

On the Lubensky-Nelson model of polymer translocation through nanopores

Peter Reimann¹ Andreas Meyer
Sebastian Getfert

Universität Bielefeld,
Fakultät für Physik, 33615 Bielefeld, Germany

¹Correspondence: reimann@physik.uni-bielefeld.de

Abstract

We revisit the one-dimensional stochastic model of Lubensky and Nelson [Biophys. J **77**, 1824 (1999)] for the electrically driven translocation of polynucleotides through α -hemolysin pores. We show that the model correctly describes two further important properties of the experimentally observed translocation time distributions, namely their spread (width) and their exponential decay. The resulting overall agreement between theoretical and experimental translocation time distributions is thus very good.

Key words: Nanopores; translocation; Stochastic modeling; Brownian motion; α -Hemolysin

Introduction

The translocation of biopolymers such as DNA, RNA, or polypeptides through protein pores plays a key role in various cellular processes (1). Apart from these biological systems, also artificial, so-called solid-state nanopores have recently attracted a lot of attention due to their promising potential as a new generation of fast and cheap DNA sequencing devices and other medical diagnostics applications (2). To achieve such goals, many experimental problems still have to be solved, and also the theoretical understanding and control of those fundamental transport processes needs substantial further development.

Here, we reconsider one of the earliest and best established theoretical models in this context, originally introduced in 1999 by Lubensky and Nelson (3), and further studied and developed in numerous subsequent works, see e.g. (4–11). Motivated by the seminal experiments on polynucleotide translocation through an α -hemolysin pore by Kasianowicz et al. (12), Lubensky and Nelson proposed a theoretical description in terms of a one-dimensional stochastic model dynamics in a tilted periodic potential (3). While many features of the experimentally observed translocation time statistics could indeed be explained remarkably well by their simple model, the theoretical spread of the translocation times underestimated the experimental one by about two orders of magnitude (3). This discrepancy was pointed out once again in the review paper (1), but to the best of our knowledge has remained a tacitly ignored problem of such a model ever since. To resolve this problem is a first main issue of our present work.

Since the quantitative details and sometimes even the qualitative findings notably depend on the considered pores and polymers, we follow Lubensky and Nelson in specifically focusing on the experimentally best studied case of the α -hemolysin protein pore and polynucleotides of single stranded DNA or RNA. In particular, for this system the translocation time distributions are quantitatively quite well documented, not only with respect to their above mentioned spread but also with respect to their decay for large times (13–16). The second main point of our paper is that the model of Lubensky and Nelson also correctly reproduces the experimentally observed exponential decay.

The overall result is a very good comparison of the complete theoretically predicted translocation time distributions with experimentally observed data sets.

Experimental System

The basic experimental set up is illustrated in Fig. 1. Charged, single-stranded polynucleotides (DNA or RNA) in aqueous solution are exposed via electrodes to an externally applied voltage. Two fluid compartments are separated by a phospholipid membrane and are connected by a single α -hemolysin protein pore. Since the phospholipid membrane is non-conducting, practically the entire voltage drop occurs within the pore and its immediate neighborhood. Whenever a polynucleotide diffusively approaches the pore from the “upper” side in Fig. 1, the electrical forces direct it into the pore and drive it to the other side of the membrane. Every such translocation process is experimentally observable as a reduction of the electrical current through the pore. Even though the polynucleotides are (practically) identical, the durations of the current blockades exhibit quite significant statistical variations. The main theoretical task is to qualitatively explain and quantitatively model the experimentally observed translocation time distributions. For further details, see, e.g., (1–16).

Model

According to Lubensky and Nelson (3), the polymer translocation process is modeled by means of a single dynamical state variable $x(t)$ (slow/relevant collective coordinate), defined as the contour length of that part of the polymer chain which already has passed through the pore until time t . In particular, hydrodynamic (dissipative) and steric (entropic) effects of the chain segments outside the pore and its immediate neighborhood are considered as negligible. The most immediate justification of this approximation is that otherwise a disagreement with the experimentally observed linear dependence of the mean translocation time upon the polymer length (1, 11, 12, 14, 15, 17, 18) seems practically unavoidable (19)¹. This general fact is nicely illustrated e.g. in Ref. (22) by means of a model very similar in spirit to the one by Lubensky and Nelson, but in addition taking into account the polymer degrees of freedom far from the pore region within an approximative, accompanying equilibrium description originally due to (23).

The state variable $x(t)$ is subjected to several kinds of forces, most notably due to the externally applied voltage and the electrostatic, mechanical,

¹While this experimental finding is beyond any doubt in the case of polynucleotide translocation through α -hemolysin pores (1, 11, 12, 14, 15, 17, 18), the corresponding results in the case of solid-state nanopores (18) are contradictory (20, 21). For this reason the Lubensky-Nelson model may be inappropriate in such a case.

and chemical interaction of the polymer with the pore walls, but also due to entropic forces within the pore and its immediate neighborhood, generated by the numerous microscopic degrees of freedom of the ambient solvent, the pore, and the polymer itself. All those forces can be considered to arise as minus the derivative of a free-energy type potential of mean force $\Phi(x)$. The remaining effects of the fast molecular degrees of freedom are approximately modeled as friction (dissipation) and noise (thermal fluctuations), while inertia effects are usually negligible on those small lengths and velocity scales. Altogether, we thus arrive at an overdamped Langevin dynamics of the well established form (24, 25)

$$\eta \dot{x}(t) = -\Phi'(x(t)) + \sqrt{2\eta kT} \xi(t) , \quad (1)$$

where $\xi(t)$ is a delta-correlated Gaussian white noise, η is the friction coefficient, and kT the thermal energy.

In the simplest case of a homopolymer, the force $-\Phi'(x)$ remains invariant when the entire polymer is translocated by the length a of one monomer, i.e. $\Phi'(x+a) = \Phi'(x)$ for all x . As a consequence, $\Phi(x)$ must be a tilted periodic potential, consisting of a strictly a -periodic part $U(x)$ and a constant “tilting” force F ,

$$\Phi(x) = U(x) - Fx . \quad (2)$$

Advancing the polymer by one monomer length a changes its (free) energy by $\Phi(x+a) - \Phi(x) = -aF$ according to Eq. 2. Following Lubensky and Nelson (3), the same change of state is obtained by moving one monomer from one to the other end of the polymer chain. The energy required for such a move is qV , where q is the charge of a monomer and V the externally applied voltage (with sign convention as indicated in Fig. 1). We thus can conclude that (3)

$$aF = -qV . \quad (3)$$

We remark that the the nominal charge per nucleotide is equal to

$$q_e = -1.602... \cdot 10^{-19} \text{ C (electron charge)}. \quad (4)$$

However, it is by now well established (26–31) that due to various electrokinetic effects of the ambient ionic solution and the pore (screening, electroosmosis, electrophoresis, polarization and field confinement mechanisms), the relevant effective charge q in Eq. 3 is reduced by roughly a factor of 10 compared to the nominal (bare) charge from Eq. 4, i.e.

$$q \approx 0.1 q_e . \quad (5)$$

Due to the above mentioned diverse effects which contribute to the charge renormalization, the exact value of q depends, among others, on temperature and ion concentrations, but also on the specific monomer (nucleotide) of which the polynucleotide is composed.

Under the assumption that V , a , and q are (approximately) known, the force F in Eq. 2 is thus fixed through Eq. 3. Much more difficult to theoretically estimate from first principles are the friction coefficient η in Eq. 1 and the periodic potential $U(x)$ in Eq. 2. They may thus be considered as a model parameter and a model function, respectively, which remain to be determined by experimental means.

Velocity and Diffusion

As a first quantity of interest we consider the average translocation velocity v of the polymer through the pore. Focusing on not too short polymers, “boundary-effects” while the polymer enters and exits the pore are negligible and v follows as the time- and ensemble-averaged velocity $\dot{x}(t)$ from the model in Eq. 1 with an infinitely extended periodic potential $U(x)$ in Eq. 2. The analytical solution of this problem goes back to Stratonovich (32) and has subsequently been rederived many times, see e.g. chapter 11 in (24). Adopting the notation from (33, 34), this solution takes the form

$$v = \frac{kT}{a\eta} \frac{1 - e^{-aF/kT}}{\int_0^a \frac{dx}{a} I(x)} , \quad (6)$$

where we have introduced

$$I(x) = e^{\Phi(x)/kT} \int_{x-a}^x \frac{dy}{a} e^{-\Phi(y)/kT} . \quad (7)$$

A further quantity of interest is the random spread of the translocation velocity (and thus of the translocation time) about its mean value v , quantified by the diffusion coefficient

$$D = \lim_{t \rightarrow \infty} \frac{\langle [x(t) - x(0) - vt]^2 \rangle}{2t} \quad (8)$$

where $\langle \cdot \rangle$ indicates an average over the noise $\xi(t)$ in Eq. 1 and over the initial positions $x(0)$.

Similarly as for the velocity v , the analytical result for the diffusion coefficient in a tilted periodic potential, Eqs. 1, 2, has been independently obtained several times. To the best of our knowledge, the first closed, exact

expression for D is buried in the paper (35). For the second time, the same problem was solved again by Lubensky and Nelson, see Appendix B in (3). Further rediscoveries are due to (36) and (33, 34). While all those results are of course equivalent, the actual formulae for D are quite different and, with the exception of (33, 34), also quite involved. For this reason, the one from (33, 34) is most common, reading

$$D = \frac{kT}{\eta} \frac{\int_0^a \frac{dx}{a} I^2(x) J(x)}{\left[\int_0^a \frac{dx}{a} I(x)\right]^3}, \quad (9)$$

where we have introduced

$$J(x) = e^{-\Phi(x)/kT} \int_x^{x+a} \frac{dy}{a} e^{\Phi(y)/kT}. \quad (10)$$

The main quantity of interest later on will be the dimensionless ratio av/D (cf. Section ‘‘Spread of Translocation Times’’ and Ref. (3)), given according to Eqs. 6 and 9 by

$$\frac{av}{D} = \frac{[1 - e^{-aF/kT}] \left[\int_0^a \frac{dx}{a} I(x)\right]^2}{\int_0^a \frac{dx}{a} I^2(x) J(x)}. \quad (11)$$

A first main result of our paper consists in the observation that the leading order behavior of Eq. 11 for small values of aF/kT takes the form

$$\frac{av}{D} \simeq \frac{aF}{kT}, \quad (12)$$

independently of any further details of the periodic potential $U(x)$. In the simplest case, this result follows by expanding the left bracket in the numerator of Eq. 11 to first (=leading) order in aF/kT and evaluating all the remaining integrals for $aF/kT = 0$ (leading=zeroth order in aF/kT). In doing so, the integrals in Eqs. 7 and 10 become x -independent and, as a consequence, the denominator in Eq. 11 becomes equal to the right bracket in the numerator. An analogous (but more tedious) expansion resulting in 12 is also contained in (3). Both expansions, however, become questionable in the weak noise limit (small thermal energy kT), since the expansion coefficients in general will inherit exponentially large values from the integrands $\exp\{\pm[U(x) - U(y)]/kT\}$ contributing via Eqs. 2, 7, 8 to the multiple integrals in 11.

Our first remark is that Eq. 12 in fact still remains valid for asymptotically weak noise ($kT \rightarrow 0$) and not too large F -values, so that the dynamics

in Eqs. 1, 2 is governed by rare, thermally activated transitions between metastable states: In this case, the dynamics can be approximately described by a one-dimensional random walk between discrete sites at distance a with certain forward and backward hopping rates r_+ and r_- , respectively. As a consequence (25), one obtains $v = a(r_+ - r_-)$ and $D = a^2(r_+ + r_-)/2$. Furthermore, detailed balance symmetry (25) implies for the forward and backward rates the relation $r_+/r_- = \exp\{aF/kT\}$. We thus obtain the asymptotically exact result

$$\frac{av}{D} = 2 \frac{1 - e^{-aF/kT}}{1 + e^{-aF/kT}} = 2 \tanh(aF/2kT) , \quad (13)$$

independently of any further details of $U(x)$. In particular, for small aF/kT one readily recovers Eq. 12.

Our second remark is that both for asymptotically large F and for asymptotically large kT , the effects of the periodic potential $U(x)$ in Eq. 2 become negligible (33, 34) with the consequence that the exact expression in Eq. 11 approaches once again the asymptotics of Eq. 12. The same conclusion is of course recovered if the variations of the periodic potential $U(x)$ itself become negligibly small.

Our last remark is that the diffusion coefficient D as a function of the tilt F develops an arbitrarily pronounced maximum for sufficiently small kT , see (33, 34). Nevertheless, closer inspection along the lines of (33, 34) shows that the ratio D/av remains a strictly decreasing function of F within the neighborhood of the maximum of D .

Translocation time distribution and exponential decay

A “successful translocation event” starts when the polymer enters the pore from one side and ends when it exits at the other side. In contrast, if the polymer exits at the same side as it entered, we are dealing with an “unsuccessful translocation attempt”. Following Lubensky and Nelson, we ignore unsuccessful attempts and henceforth only consider the successful events. Regarding the experimental identification of such events see e.g. (16). The statistical distribution of their duration is the quantity of foremost interest from now on.

A main achievement of Lubensky and Nelson’s work (3) is an analytical approximation for the distribution (probability density) $\psi(t)$ of translocation times. In fact, the approximation becomes asymptotically exact for

sufficiently large numbers N of monomers, i.e.

$$N = L/a \gg 1, \quad (14)$$

where a and L denote the lengths of one monomer and of the entire polymer, respectively.

Remarkably enough, but also quite plausible at second glance, the only parameters entering the translocation time distribution $\psi(t)$ are the polymer length L and the velocity v and diffusion coefficient D of the corresponding, infinitely extended dynamics. Furthermore, it is convenient to employ the rescaled, dimensionless time

$$\tau = \frac{vt}{L} \quad (15)$$

and the dimensionless auxiliary parameter

$$\kappa = \frac{4D}{vL}. \quad (16)$$

Referring to Appendix A of (3) for the detailed calculations, the final analytical expression provided by eq. (A6) in (3) and can be rewritten in the form

$$\psi(t) = \frac{c}{\tau^{3/2}} \sum_{n=1,3,5,\dots} \frac{\frac{n^2}{\kappa\tau} - \frac{1}{2}}{\exp\left\{\frac{2(n-1)}{\kappa} + \frac{(\tau-n)^2}{\kappa\tau}\right\}} \quad (17)$$

where the normalization constant c is given by²

$$c = \frac{v}{L} \sqrt{\frac{\kappa}{\pi}} [1 - e^{-4/\kappa}]. \quad (18)$$

In other words, the translocation time distribution $\psi(t)$ actually does not depend separately on all three parameters L , v , and D , but only on the two specific combinations v/L and $\kappa = 4D/vL$.

The behavior of Eq. 17 for large t is not obvious at all. In particular, for large τ the summands on the right hand side are negative up to quite large n -values, while those for even larger n are positive. In view of the property $\psi(t) \geq 0$ and the expected asymptotics $\psi(t) \rightarrow 0$ for $t \rightarrow \infty$, there must be a very fragile cancellation of positive and negative summands. On the other hand, we observe that, according to eq. (A2) in (3), an asymptotically exponential decay of the right hand side in Eq. 17 may be conjectured with a decay rate

$$\lambda = (\pi/2)^2 \kappa + 1/\kappa. \quad (19)$$

²There is a typo on the right hand side of eq. (A6) in (3): the first factor 2 should be replaced by 1/2

In view of this surmise, we thus may rewrite Eq. 17 in the following equivalent form

$$\psi(t) = c' g(\kappa \tau) e^{-\lambda \tau} , \quad (20)$$

where c' is another normalization constant, and where the auxiliary function $g(x)$ is defined as follows

$$g(x) = 0.45731 \frac{e^{x\pi^2/4}}{x^{3/2}} \sum_{n=1,3,5,\dots} \frac{\frac{n^2}{x} - \frac{1}{2}}{e^{n^2/x}} . \quad (21)$$

As can be seen from Fig. 2, the function $g(x)$ converges towards a finite limit for $x \rightarrow \infty$ and the specific numerical factor 0.45731 in Eq. 21 has been chosen so that this limit is (practically) unity.

This brings us to the next main result of our paper: According to Eq. 20 and Fig. 2, the distribution of translocation times $\psi(t)$ predicted by the model of Lubensky and Nelson exhibits an exponential decay for large times, in agreement with the experimental findings from (13–16).

We finally remark that equation 20 together with Fig. 2 and Eqs. 15, 16, 19 provide a quite detailed qualitative picture of the translocation time distribution $\psi(t)$, and how it depends on the parameters v/L and κ : Initially, $\psi(t)$ remains close to zero, then increases quite steeply up to a maximum at $t_{max} = \tau_{max}L/v$, where τ_{max} solves $\kappa g'(\kappa\tau_{max}) = \lambda g(\kappa\tau_{max})$, and finally approaches an exponential decay.

Numerically, for any given set of parameters v/L and κ the quantitative evaluation of $\psi(t)$ according to Eqs. 15-18 is straightforward. In particular, for $\kappa \rightarrow 0$ (vanishing thermal fluctuations) one recovers the expected deterministic limit $\psi(t) \rightarrow \delta(t - L/v)$. Typical examples will be presented in Section “Comparison with Experiments” below.

Spread of translocation times

Concerning a quantitative comparison between the theoretical prediction from Eq. 17 and experimental data, we first observe that there are two fit parameters: One (namely L/v in Eq. 15) amounts to a quite trivial rescaling of time, which can be readily fixed e.g. by fitting the theoretical peak of $\psi(t)$ to the experimentally observed one. The remaining, second fit parameter is κ from Eq. 16, which can be determined by the following very convenient procedure originally due to Lubensky and Nelson (3): In a first step, the peak position t_{max} of the experimentally observed $\psi(t)$ is

determined, formally defined via $\psi'(t_{max}) = 0$. Then the two times t_L and t_R to the left (L) and to the right (R) of t_{max} are determined according to

$$\psi(t_{L,R}) = e^{-1/2} \psi(t_{max}) \simeq 0.606 \cdot \psi(t_{max}) . \quad (22)$$

In other words, $t_R - t_L$ quantifies the width of the experimentally observed peak of $\psi(t)$. Observing that the ratio $(t_R - t_L)/t_{max}$ is independent of the chosen units of time, we can readily recast the approximative relation from Fig. 3 of Lubensky and Nelson's work (3) into the form $(t_R - t_L)/t_{max} \simeq \sqrt{2\kappa}$. In fact, this approximation becomes exact for asymptotically small $(t_R - t_L)/t_{max}$ and remains quite accurate as long as $(t_R - t_L)/t_{max} \leq 1$. In other words, we obtain the quite accurate estimate

$$\kappa \simeq \frac{1}{2} \left(\frac{t_R - t_L}{t_{max}} \right)^2 \quad \text{provided} \quad \frac{t_R - t_L}{t_{max}} \leq 1 . \quad (23)$$

On the other hand, combining Eqs. 3, 12, 14, and 16 yields the relation

$$\frac{kT}{(-q)V} \simeq \frac{\kappa N}{4} \quad \text{provided} \quad \frac{\kappa N}{4} \geq 1 . \quad (24)$$

From the experimental data in Fig. 2 of Kasianowicz et al. (12) one readily reads off $(t_R - t_L)/t_{max} \simeq 1$ (3), implying with Eq. 23 that $\kappa \simeq 0.5$. Taking into account that $N = 210$ in the experiments from (12), the right hand side of Eq. 24 amounts to $\kappa N/4 \simeq 26$. Hence the condition $\kappa N/4 \geq 1$ is fulfilled and we can apply Eq. 24 to conclude that $kT/qV \simeq 26$. On the other hand, using $T \simeq 293$ K (room temperature), $V = 120$ mV (experimental voltage from (12)), and the nominal charge $q = q_e \simeq -1.6 \cdot 10^{-19}$ C per nucleotide from (3), we obtain the result $kT/(-q)V \simeq 0.21$. In view of the discrepancy with the relation $kT/(-q)V \simeq 26$ following from Eq. 24, Lubensky and Nelson concluded that their model, Eq. 1, which implied Eq. 24, was inconsistent with the experimental facts.

In the following, we argue that this conclusion is not tenable. Rather, the prediction from Eq. 24 of the model, Eq. 1, agrees quite well with the experimental findings. To this end, we first evaluate the right hand side of Eq. 24 by means of the results from several more recent, and therefore possibly more accurate experiments than in the original work of Kasianowicz et al. (12): From the two data sets of Meller et al. displayed in Fig. 2 of their work (13) (see also Fig. 3 in (14) and Fig. 6 in (15)) one can infer with Eq. 23 that $\kappa \simeq 0.09$ and $\kappa \simeq 0.11$, respectively (see also next Section). With $N = 100$ (13) it follows that $\kappa N/4 \simeq 2.3$ and $\kappa N/4 \simeq 2.8$, respectively. Likewise, one can infer from the data in Fig. 2 of Bates et al. (37) that

$\kappa \simeq 0.17$ and hence with $N = 60$ that $\kappa N/4 \simeq 2.6$. Finally the data from Fig. 5 of Butler et al. (16) imply that $\kappa \simeq 0.19$ and with $N = 50$ that $\kappa N/4 \simeq 2.4$.

We remark that in all those experiments homopolymers have been used and that we do not know of any further data of this kind (histograms of translocation durations for homopolymers) in the literature. For the sake of completeness, we may also include here the data for heteropolymers with $N = 92$ from Fig. 2c in Maglia et al. (38), yielding $\kappa = 0.13$ and hence $\kappa N/4 \simeq 3.0$.

Turning to the quantity $kT/(-q)V$ appearing on the left hand side of Eq. 24, we observe that the voltage $V = 120$ mV, and the temperature $T \simeq 293$ K was (approximately) the same in all the experiments from (12–16, 37, 38). Using the nominal charge $q = q_e$ per nucleotide from (3), one thus recovers the same result $kT/(-q)V \simeq 0.21$ as before, and hence Eq. 24 still seems to be violated. However, according to (26–31) a much more realistic estimate follows by employing the appropriately renormalized effective charge from Eq. 5, namely $kT/(-q)V \simeq 2.1$. As a consequence, the theoretically predicted relation in Eq. 24 is satisfied quite well by all the more recent pertinent experiments (13–16, 37, 38).

Taking the model of Lubensky and Nelson and thus Eq. 24 for granted, the above findings for $\kappa N/4$ may now in turn be used to estimate the renormalized charge q more accurately than in Eq. 5. Since temperature, voltage, buffer etc. were almost the same in all cases, the resulting differences in q must be mainly due to the different nucleotides (see also below Eq. 5).

With respect to the earlier experiment by Kasianowicz et al. (12), a further reduction of the effective charge by another factor of 10 would be a possible, though not very satisfying, explanation (see also next Section). A more likely reason seems to be connected with the considerably larger $\kappa N/4$ -value compared to the more recent experiments. In other words, the experimentally observed spread of the translocation times is unusually large. Indeed, one generally expects that the experimentally observed spreads of the translocation times still somewhat overestimate the purely diffusive effects accounted for in the theory. One possible reason of why the observed spread was particularly large in (12) may be that the data analysis and pre-processing according to their detailed current blockade signatures was not yet as sophisticated as e.g. in (13–16). Another possible factor is the smaller measurement bandwidth of about 24 KHz for the experiments (12), compared to 100 KHz for (13–15, 37) and 50 KHz for (16). As will be argued in the next section, the most plausible explanation is a relatively large spread of the polynucleotide lengths of the samples used by Kasianowicz et

al. (12).

Comparison with experiments

The purpose of this Section is a comparison between the complete translocation time distributions for several of the experiments already considered in the previous Section and the corresponding theoretical distributions. Quite surprisingly, such a detailed quantitative comparison does not seem to exist in the previous literature known to us.

As a first example, Fig. 3 presents the experimental data reported by Butler et al. (16) for single-stranded RNA rC_{50} polynucleotides (i.e. $N = 50$ in Eq. 14). The theoretical translocation time distribution has been obtained as described in the previous Section: First, one readily reads off from the experimental data points that $(t_R - t_L)/t_{max} \simeq 0.61$, yielding with Eq. 23 the estimate $\kappa \simeq 0.19$. Then, the time-scale parameter L/v in Eq. 15 is adapted so as to optimally fit the peak position of the experimental data, resulting in the estimate $L/v \simeq 0.2$ ms. According to Fig. 3, the theoretical $\psi(t)$ obtained in this way agrees very well with the experimental findings with the exception of the times t smaller than about 0.1 ms. In fact, the corresponding experimental data were denoted in Ref. (16) as “ambiguous signals”, possibly caused by “retraction of the threaded configuration back into the vestibule configuration, very rapid translocation, or translocation of short polynucleotide fragments. Due to the ambiguity in the interpretation of these short Deep states, we only designated Deep states with durations longer than the minimum as translocations.” This ambiguity in the interpretation of the experimental current blockades (“Deep states”) seems to us a sufficiently convincing explanation of the deviations from the theoretical curve at small times t . An apparently rather similar situation for small t has in fact been discussed already in (3, 12, 42). In view of this ambiguity for $t < 0.1$ ms we fitted in Fig. 3 the scaling factor c of the theoretical curve 17 as well as possible to the experimental data for $t > 0.1$ ms rather than normalizing it according to 18.

As a second example, Fig. 4 shows the data of Bates et al. (37) for single-stranded DNA dA_{60} polynucleotides (i.e. $N = 60$ in Eq. 14). Theoretically, we proceeded as before with $(t_R - t_L)/t_{max} \simeq 0.58$, $\kappa \simeq 0.17$, and $L/v \simeq 0.42$ ms. Again, the overall agreement between theory and experiment is very nice with the exception of large times t^3 .

³In fact, the authors of Ref. (37) mention that the tail of the experimentally observed distribution extends to even much longer times without providing the actual data.

As pointed out by an anonymous referee, the latter disagreement can be naturally explained by the well-known directionality of the polynucleotide’s sugar-phosphate backbone, resulting in two different translocation time distributions depending on whether the DNA enters the pore with its 3’ or 5’ end first (3, 12, 16, 39–45). Denoting the probabilities of 3’ and 5’ entries by p and $1 - p$ and the concomitant two distributions by $\psi_1(t)$ and $\psi_2(t)$, the total (experimentally observed) distributions is given by

$$\psi(t) = p\psi_1(t) + (1 - p)\psi_2(t) . \quad (25)$$

Within the model of Lubensky and Nelson, $\psi_1(t)$ and $\psi_2(t)$ are both of the form 17. For both of them, the parameter κ must be the same according to Eqs. 3, 12, 16 under the plausible assumption that the effective charge q is (approximately) the same for both DNA orientations (see also below Eq. 5). On the other hand, there may in general be two different time scales L/v_1 and L/v_2 , and likewise for τ in Eq. 15. Along these lines, the best fit to the experimental data of Bates et al. (37) was obtained for $\kappa \simeq 0.18$, $L/v_1 \simeq 0.42$ ms, $L/v_2 \simeq 0.82$ ms, and $p \simeq 0.81$. According to Fig. 5, the resulting agreement between experiment and theory is indeed very good. We remark that while quantitative experimental estimates for the two “extra parameters” p and v_1/v_2 of the extended theory 25 do not seem available, the “event diagrams” for dA_{50} in Fig. 3 of the paper (16) and for dA_{100} in Fig. 2 of the paper (40) qualitatively compare very favorably with our above findings $p \simeq 0.81$ and $v_1/v_2 \simeq 2$ for dA_{60} . We finally remark that also in the works (13, 40) two “groups” of dA_{100} translocation events were identified, “group 1” containing about 80% of the events (at 20° C) (13), and that the two “groups” can be attributed to the two different DNA orientations (40, 42).

As expected, the already very good agreement in Fig. 3 with the rC_{50} data by Butler et al. (16) could not be notably improved any more by means of the extended theory from Eq. 25. This is consistent with the “event diagram” for rC_{50} in Fig. 3 of the paper (16), evidencing that while the RNA may indeed again exhibit two different orientations, the translocation time distributions happen to be very similar for both of them.

We finally return to the experiment of Kasianowicz et al. (12), using poly[U] samples with a nominal length of $N = 210$ nucleotides. In a later work (39), the same group used a poly[U] sample whose length distribution was specified as $N = 150 \pm 50$ nucleotides. According to a personal communication by one of the authors (D. Branton, Harvard University), a comparable polydispersity of $N = 210 \pm 70$ may thus be considered as quite

plausible also in the earlier work (12). Theoretically, we took into account this fact by including on the right hand side of Eq. 25 an integral over a Gaussian length distribution. Formally, this is achieved by replacing L in the definitions 15 and 16 by zL , where $z > 0$ is Gaussian distributed⁴ with average 1 and standard deviation $1/3$, and likewise for the two time scales L/v_1 , L/v_2 entering into Eq. 25. Fig. 6 shows our best fit to the experimental data of Kasianowicz et al. (12), obtained for $\kappa \simeq 0.1$, $L/v_1 \simeq 0.31$ ms, $L/v_2 \simeq 1.3$ ms, and $p \simeq 0.58$. The agreement is obviously very good, except for the leftmost data point in Fig. 6. In fact, there are additional experimental data points at even smaller t -values with ψ -values beyond the range displayed in Fig. 6. Similarly as in Fig. 3, they are commonly considered to be due to polymers that partially entered the channel but then retracted rather than actually traversed the channel (3, 12, 16, 42). Such events are not covered by our present theory, explaining the disagreement in Fig. 6 at small t . Accordingly, the experimental data in Fig. 6 have not been normalized to unity but rather so that the agreement with the theory was optimal.

We remark that such “unsuccessful translocation attempts” could be sorted out in the experimental data in Figs. 4 and 5 thanks to their very specific current blockade signatures (37). Hence the theory explains the data even at small t . A similar identification of such events in the experiments by Kasianowicz et al. (12) and by Butler et al. (16) was apparently not possible.

Returning to Fig. 6, the obtained fit $\kappa = 0.1$ implies that $\kappa N/4 = 5.25$ and thus with Eqs. 24 and 4 that $q \approx 0.04q_e$. Such an effective charge is smaller than the estimate from equation 5 but still reasonably close to our previously obtained q -values⁵. We also remark that by assuming a larger polydispersity of $N = 210 \pm 95$, the data from Fig. 6 could be fitted practically equally well but now with $\kappa = 0.05$ and hence $q \approx 0.08q_e$, and likewise for $N = 210 \pm 120$ and any $q > 0.5q_e$. In contrast, without any polydispersity the best fit becomes somewhat worse than in Fig. 6 and $q \approx 0.015q_e$ becomes unrealistically small.

Finally, we also fitted the above extended model to the experimental data sets from Figs. 3 and 5 but for any non-negligible polydispersity this always resulted in a less good agreement than without any polydispersity.

⁴Since $z \leq 0$ is ruled out, the Gaussian must be truncated and properly renormalized.

⁵Note that also the “blocking currents” may vary substantially for different nucleotides and that this may be closely related to variations of q (27).

Discussion

In their seminal work (3), Lubensky and Nelson showed that their simple one-dimensional stochastic model, Eqs. 1-3, captures many of the experimental observations on polynucleotide translocation through α -hemolysin nanopores. However, the quantitative behavior of the experimental translocation time distribution of Kasianowicz et al. (12) could not be satisfactorily explained. Here, we resolved this long standing problem by taking into account that due to various electrokinetic effects the relevant effective charge of the nucleotides is substantially reduced compared to their bare (nominal) charge.

A second main point of our work was to show that the model of Lubensky and Nelson implies an asymptotically exponential decay of the translocation time distribution, in agreement with the experimental results from Refs. (13–16).

Finally, we compared the complete theoretically predicted translocation time distributions with experimental distributions from the literature. Taking into account the directionality of polynucleotides, the non-negligible polydispersity in the experiment by Kasianowicz et al. (12), and the fact that “unsuccessful translocation attempts” are not covered by the theory, the model of Lubensky and Nelson explains the experimental observations remarkably well.

Regarding alternative, more sophisticated descriptions e.g. in term of bead-spring models with many degrees of freedom (19), one naturally expects that – at least within certain regimes or limits of the various model parameters – the main features of the one-dimensional model of Lubensky and Nelson should be recovered. Particularly important such features are the experimentally observed linear dependence of the mean translocation time upon the polymer length (see also Section “Model”) and the main quantitative characteristics of the observed translocation time distributions, most notably their spread and exponential decay. The essential open question with respect to those more sophisticated models is then, whether the numerous extra degrees of freedom in order to describe the hydrodynamic and entropic effects outside the immediate pore region still play a significant role within the above mentioned, relevant model parameter regimes.

We thank D. Branton for a very helpful e-mail exchange regarding Ref. (12). This work was supported by Deutsche Forschungsgemeinschaft under SFB 613 and RE1344/8-1.

References

1. Meller, A. 2003. Dynamics of polynucleotide transport through nanometre-scale pores. *J. Phys.: Condens. Matter* 15:R581-R607.
2. Venkatesan, B. M., and R. Bashir. 2011. Nanopore Sensors for Nucleic Acid Analysis. *Nature Nanotech.* 6:615-624.
3. Lubensky, D. K., and D. R. Nelson. 1999. Driven polymer translocation through a narrow pore. *Biophys. J.* 77:1824-1838.
4. Kafri, Y, D. K. Lubsenky, and D. R. Nelson. 2004. Dynamics of molecular motors and polymer translocation with sequence heterogeneity. *Biophys. J.* 86:3373-3391.
5. Lua, R. C., and A. Y. Grosberg. 2005. First passage times and asymmetry of DNA translocation. *Phys. Rev. E* 72:061918-1-8.
6. Wanunu, M., B. Chakrabarti, J. Mathé, D. R. Nelson, and A. Meller. 2008. Orientation-dependent interactions of DNA with an α -hemolysin channel. *Phys. Rev. E* 77:031904-1-5.
7. Chen, Z., Y. Jiang, D. R. Dunphy, D. P. Adams, C. Hodges, N. Liu, N. Zhang, G. Xomeritakis, X. Jin, N. R. Aluru, S. J. Gaik, H. W. Hillhouse, C. J. Brinker. 2010. DNA translocation through an array of kinked nanopores. *Nat. Mat.* 9:667-675.
8. Li, J., and D. S. Talaga. 2010. The distribution of DNA translocation times in solid-state nanopores. *J. Phys.: Condens. Matter* 22:454129-1-8.
9. Lu, B., F. Albertorio, D. P. Hoogerheide, and J. A. Golovchenko. 2011. Origins and consequences of velocity fluctuations during DNA passage through a nanopore. *Biophys. J.* 101:70-79.
10. Muthukumar, M. 2010. Theory of capture rate in polymer translocation. *J. Chem. Phys.* 132:195101-1-10.
11. Wong, C. T. A., and M. Muthukumar. 2010. Polymer translocation through α -hemolysin pore with tunable polymer-pore electrostatic interaction. *J. Chem. Phys.* 133:045101-1-12.
12. Kasianowicz, J. J., E. Brandin, D. Branton, and D. W. Deamer. 1996. Characterization of individual polynucleotide molecules using a membrane channel. *PNAS* 93:13770-13773.

13. Meller, A., L. Nivon, E. Brandin, J. Golovchenko, and D. Branton. 2000. Rapid nanopore discrimination between single polynucleotide molecules. *PNAS* 97:1079-1084.
14. Meller, A., L. Nivon, and D. Branton. 2001. Voltage-driven DNA translocation through a Nanopore. *Phys. Rev. Lett.* 86:3435-3438.
15. Meller, A., and D. Branton. 2002. Single molecule measurements of DNA transport through a nanopore. *Electrophoresis* 23:2583-2591.
16. Butler, T. Z., J. H. Gundlach, and M. A. Troll. 2007. Ionic current blockades from DNA and RNA molecules in the α -hemolysin nanopore. *Biophys. J.* 93:3229-3240.
17. Deamer, D. W., and D. Branton. 2002. Characterization of nucleic acids by nanopore analysis. *Acc. Chem. Res.* 35:817-825.
18. Dekker, C. 2007. Solid-state nanopores. *Nat. Nanotechnol.* 2:209-215.
19. Milchev, A. 2011. Single-polymer dynamics under constraints: scaling theory and computer experiment. *J. Phys.: Condens. Matter* 23:103101-1-24.
20. Chen, P., J. Gu, E. Brandin, Y.-R. Kim, Q. Wang, and D. Branton. 2004. Probing single DNA molecule transport using fabricated nanopores. *Nano Lett.* 4:2293-2298.
21. Storm, A. J., C. Storm, J. Chen, H. Zandbergen, J.-F. Joanny, and C. Dekker. 2005. Fast DNA translocation through a solid-state nanopore. *Nano Lett.* 5:1193-1197.
22. Muthukumar, M. 1999, Polymer translocation through a hole. *J. Chem. Phys.* 111:10371-10374.
23. Sung, W., and Park, P. J. 1996. Polymer Translocation through a pore in a Membrane. *Phys. Rev. Lett.* 77:783-786.
24. H. Risken, *The Fokker-Planck Equation*, Springer, Berlin, 1984.
25. Reimann, P. 2002. Brownian Motors: Noisy Transport far from Equilibrium. *Phys. Rep.* 361:57-265.

26. Rabin, Y., and M. Tanaka. 2005. DNA in nanopores: counterion condensation and coion depletion. *Phys. Rev. Lett.* 94:148103-1-4.
27. Zhang, J., and B. I. Shlokovskii. 2007. Effective charge and free energy of DNA inside an ion channel. *Phys. Rev. E* 75:021906-1-10.
28. Ghosal, S. 2007. Effect of salt concentration on the electrophoretic speed of a polyelectrolyte through a nanopore. *Phys. Rev. Lett.* 98:238104-1-4.
29. Henrickson, S. E., M. Misakian, B. Robertson, and J. J. Kasianowicz. 2000. Driven DNA transport into an asymmetric nanometer-scale pore. *Phys. Rev. Lett.* 85:3057-3060.
30. Luo, K., T. Ala-Nissila, S.-C. Ying, and A. Bhattacharya. 2008. Sequence dependence of DNA translocation through a nanopore. *Phys. Rev. Lett.* 100:058101-1-4.
31. Brun, L., M. Pastoriza-Gallego, G. Oukhaled, J. Mathé, L. Bacri, L. Auvray, and J. Pelta. 2008. Dynamics of polyelectrolyte transport through a protein channel as a function of applied voltage. *Phys. Rev. Lett.* 100:158302-1-4.
32. Stratonovich, R. L. 1958. Oscillator synchronization in the presence of noise, *Radiotekhnika i elektronika* 3:497. English translation in *Non-linear transformations of stochastic processes*. P. I. Kuznetsov, R. L. Stratonovich, V. I. Tikhonov, editors. Pergamon, Oxford, 1965.
33. Reimann, P., C. Van den Broeck, H. Linke, P. Hänggi, J. M. Rubi, and A. Pérez-Madrid. 2001. Giant Acceleration of Free Diffusion by Use of Tilted Periodic Potentials. *Phys. Rev. Lett.* 87:010602:1-4.
34. Reimann, P., C. Van den Broeck, H. Linke, P. Hänggi, J. M. Rubi, and A. Pérez-Madrid. 2002. Diffusion in tilted periodic potentials: Enhancement, universality, and scaling. *Phys. Rev. E* 65:031104-1-16.
35. Parris, P. E., M. Kus, D. H. Dunlap, and V. M. Kenkre. 1997. Nonlinear response theory: Transport coefficients for driving fields of arbitrary magnitude. *Phys. Rev. E* 56:5295-5305.

36. Lindner, B., M. Kostur, and L. Schimansky-Geier. 2001. Optimal diffusive transport in a tilted periodic potential. *Fluct. Noise Lett.* 1:R25-R39.
37. Bates, M., M. Bruns, and A. Meller. 2003. Dynamics of DNA molecules in a membrane channel probed by active control. *Biophys. J* 84:2366-2372.
38. Maglia, G., M. R. Restrepo, E. Mikhailova, and H. Bayley. 2008. Enhanced translocation of single DNA molecules through α -hemolysin nanopores by manipulation of internal charge. *PNAS* 105:19720-19725.
39. Akeson, M., D. Branton, J. J. Kasianowicz, E. Brandin, and D. W. Deamer. 1999. Microsecond time-scale discrimination among polycytidylic acid, polyadenylic acid, and polyuridylic acid as homopolymers or as segments within single RNA molecules. *Biophys. J.* 77:3227-3227.
40. Wang, H., J. E. Dunning, A. P.-H. Huang, J. A. Nyamwanda, and D. Branton. 2004. DNA heterogeneity and phosphorylation unveiled by single-molecule electrophoresis. *PNAS* 101:13472-13477.
41. Mathé, J., A. Aksimentiev, D. R. Nelson, K. Schulten, and A. Meller. 2005. Orientation discrimination of single stranded DNA inside the α -hemolysin membrane channel. *PNAS* 102:12377-12382.
Butler,
42. Butler, T. Z. , J. H. Gundlach, and M. A. Troll. 2006. Determination of RNA orientation during translocation through a biological nanopore. *Biophys. J.* 90:190-199.
43. Purnell, R. F., K. K. Mehta, and J. J. Schmidt. 2008. Nucleotide identification and orientation discrimination of DNA homopolymers immobilized in a protein nanopore. *Nano Lett.* 8:3029-3034.
44. Muzard, J., M. Martinho, J. Mathé, U. Bockelmann, and V. Viasnoff. 2010. DNA translocation and unzipping through a Nanopore: some geometrical effects. *Biophys. J.* 98:2170-2178.
45. Aksimentiev, A. 2010. Deciphering ionic current signatures of DNA transport through a nanopore. *Nanoscale* 2:468-483.

Figure Legends

Figure 1

Schematic illustration of the experimental set up: polynucleotide chains (single-stranded DNA or RNA) translocate through an α -hemolysin protein pore due to the externally imposed voltage difference between the electrodes.

Figure 2

The function $g(x)$ obtained by numerically evaluating Eq. 21.

Figure 3

Line: Theoretical translocation time distribution $\psi(t)$ according to Eqs. 15-18 with $\kappa = 0.19$ and $L/v = 0.2$ ms. Symbols: Experimentally observed translocation times, adopted from Fig. 5 of Butler et al. (16).

Figure 4

Line: Theoretical translocation time distribution $\psi(t)$ according to Eqs. 15-18 with $\kappa = 0.17$ and $L/v = 0.42$ ms. Symbols: Experimentally observed translocation times, adopted from Fig. 2 of Bates et al. (37).

Figure 5

Line: Theoretical translocation time distribution $\psi(t)$ according to Eqs. 25 (see also main text for details) with $\kappa = 0.18$, $L/v_1 = 0.42$ ms, $L/v_2 = 0.82$ ms, and $p = 0.81$. Symbols: Experimentally observed translocation times, adopted from Fig. 2 of Bates et al. (37).

Figure 6

Line: Theoretical translocation time distribution $\psi(t)$, accounting for polydispersity by randomizing Eqs. 25 (see main text) with $\kappa = 0.1$, $L/v_1 = 0.31$ ms, $L/v_2 = 1.3$ ms, $p = 0.58$. Symbols: Experimentally observed translocation times, adopted from Fig. 2 of Kasianowicz et al. (12).

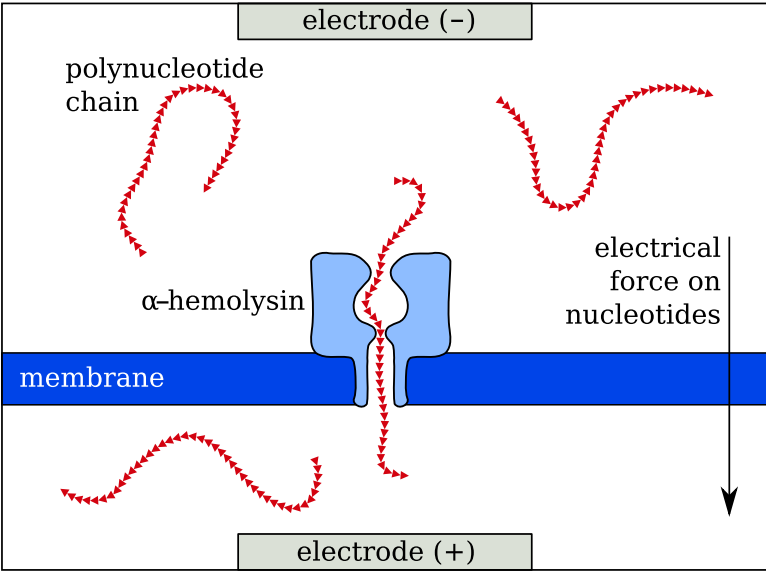


Figure 1:

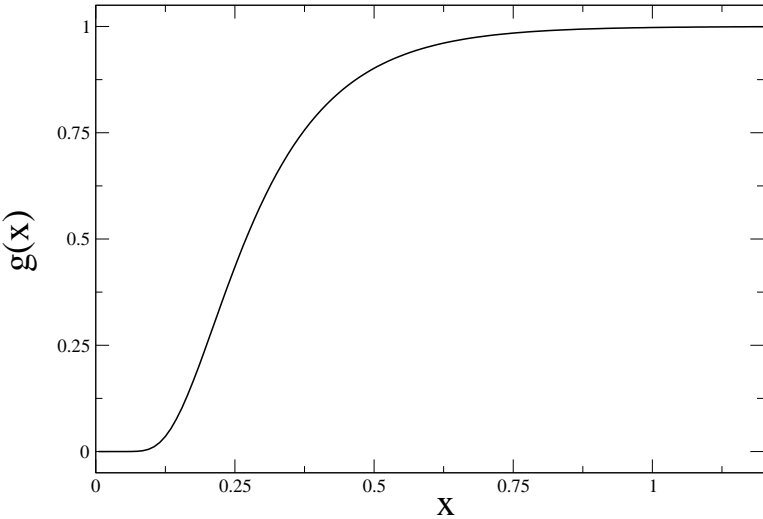


Figure 2:

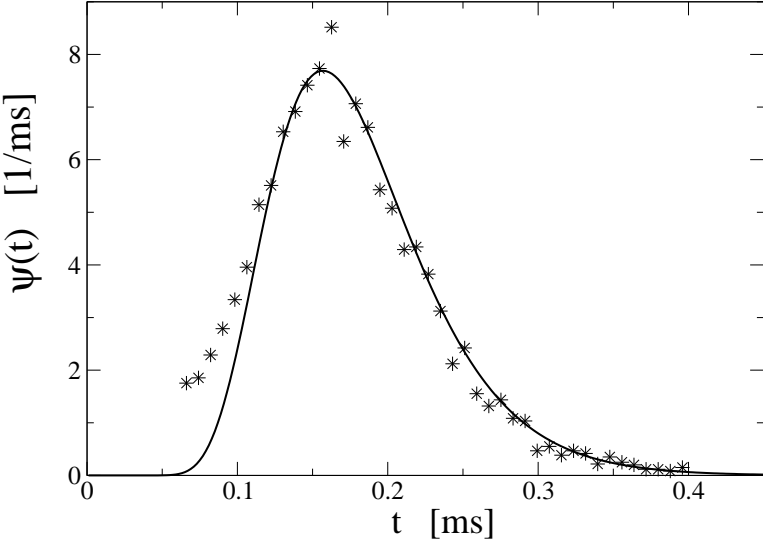


Figure 3:

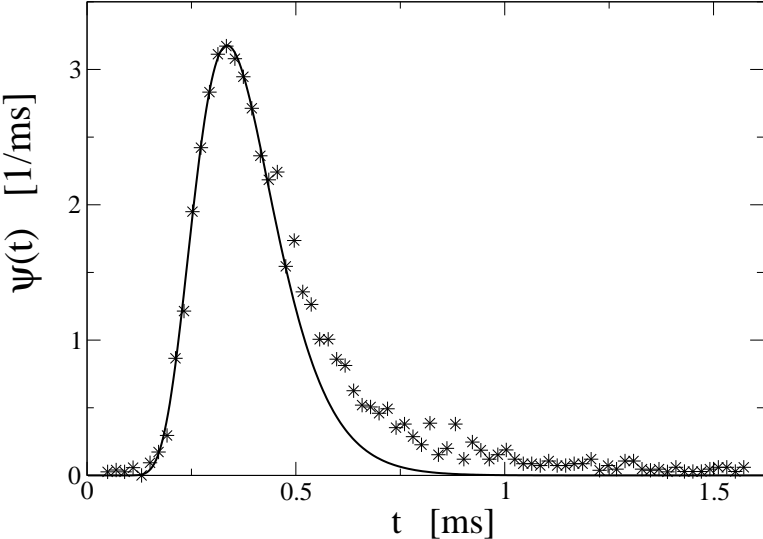


Figure 4:

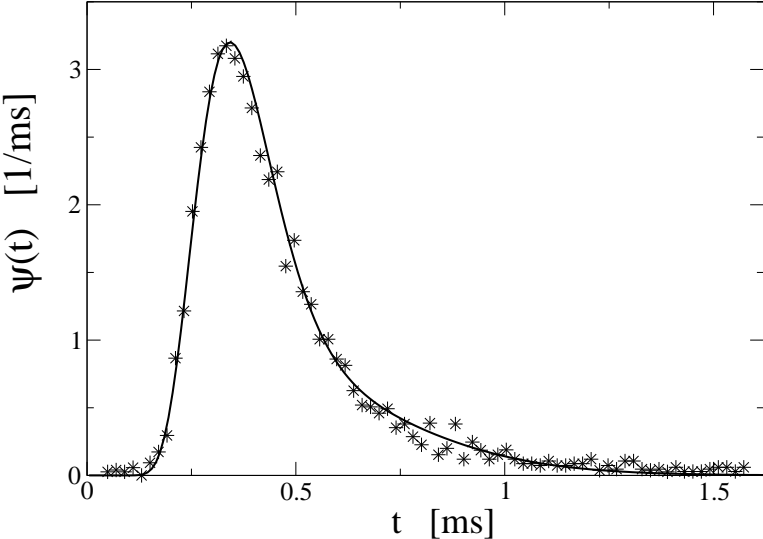


Figure 5:

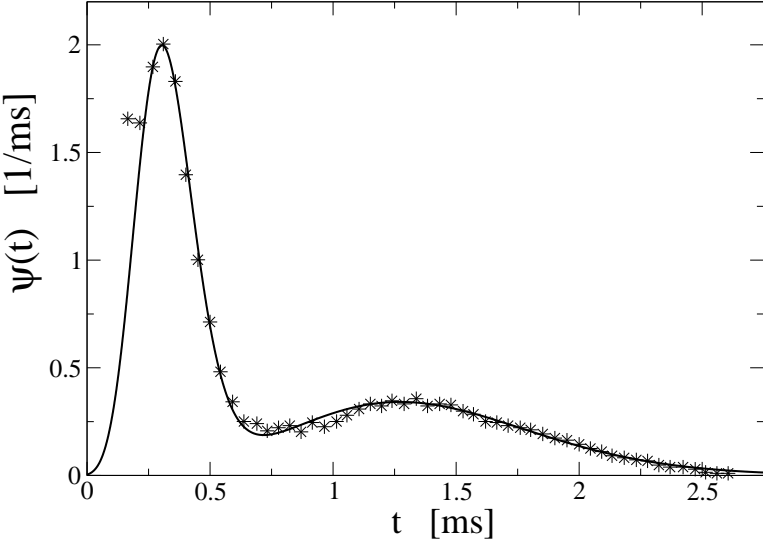


Figure 6: